A 6-ka climatic cycle during at least the last 50,000 years

LARS OLSEN & ØYVIND HAMMER

Olsen, L. & Hammer, Ø. 2005: A 6-ka climatic cycle during at least the last 50,000 years. *Norges geologiske undersøkelse Bulletin 445*, 89–100.

The distribution of 264 dates in the interval 12,000 – 50,000 years BP from terrestrial and raised marine sediments from ice-free intervals in Norway shows a fairly strong cycle with a period of c. 6 thousand years. The cycle, or semi-cycle (*sensu stricto*) is supported by spectral analysis and autocorrelation. The latter indicates statistical significance for a 6 ka cycle at probability $p<0.05$. The spectral peak for the same periodicity is relatively strong, but still not fully statistically significant in the interval 11,000–32,000 (^{14}C) years BP. The ice-free intervals are separated by ice growth intervals of different length. Some of these appear to have had a very short duration and a diachronous character, which would reduce the statistical significance of the spectral peak. The number of dates from each ice-free interval may be partly a reflection of the organic growth conditions, but is also simply a result of availability (natural sections, excavations, etc.). The timing and duration of the intervals of glacial growth and ice-free conditions may be a result of a number of linkages and feedbacks within the climate system. The causal mechanisms for the observed periodicity are a matter of discussion, but are not likely to be limited only to the internal processes in the Earth's climatic system. This conclusion is strengthened when data from the Holocene is added. External forcing, such as periodic changes in the magnetic field or other astronomical mechanisms, is probably also involved and is perhaps even the main cause. Finally, we realize that the present published terrestrial data give no basis for evaluation of how far back in time prior to 50 ka BP the observed climatic cycle of c. 6 ka may have been valid, but the published record from ice cores and marine sediments suggests that such a cycle may be traced at least back to c. 90 ka BP.

Lars Olsen, Norges geologiske undersøkelse, N-7491 Trondheim, Norway; Øyvind Hammer, Geological Museum, Boks 1172 Blindern, N-0318 Oslo, Norway.
E-mail addresses: lars.olsen@ngu.no (for dates and glacial variations); and oyvind.hammer@nhm.uio.no (for statistical treatment and spectral analysis).

Introduction

Large, millennial-scale climatic shifts occurred repeatedly in many parts of the Northern Hemisphere during the Last Glacial period, particularly from about 75,000 to 12,000 years ago. These are recorded in different manner, e.g., by oxygen isotope fluctuations known as Dansgaard – Oeschger (DO) cycles in Greenland ice cores (Grootes et al. 1993; Stuiver & Grootes 2000); by microfauna, isotopes and magnetic susceptibility in sediment cores from various marine basins including the North Atlantic (Bond et al. 1993, Rasmussen et al. 1996, Marchitto et al. 1998, Sachs & Lehman 1999, van Kreveld et al. 2000), the tropical Atlantic Cariaco Basin (Hughen et al. 1996; Peterson et al. 2000), the Mediterranean (Cacho et al. 1999), the Pacific outside California (Kennett et al. 2000, Hendy et al. 2002), and the Arabian Ocean (Altabet et al. 2002); and by particle size variations in loess from northern China and marine sediment from the Sea of Japan (Porter & An 1995, Tada & Irino 1999).

Wang et al. (2001) showed that climatic oscillations reflected in $\delta^{18}O$ from stalagmites from eastern China correlate well with the DO events 1-21, indicating a strong correspondence between the East Asian Monsoon intensity and the Greenland air temperature. Gentry et al. (2003) found rapid climatic oscillations in $d^{18}O$ and $d^{13}C$ from a stalagmite from southwestern France. These oscillations corresponded with the DO events between 83,000 and 32,000 years BP.

Benson et al. (2003) studied changes in the sediments of four lakes in the Great Basin area of North America. They showed that these lakes responded relatively distinctly to the DO events 2-12. Ice cores from southern areas of the world have revealed variations which indicate that DO cycles also occur in such records from the Southern Hemisphere (Hinnov et al. 2002).

As seen in the Greenland ice cores, a typical DO cycle has an average period of c. 1500-2500 years, with a relatively long cold phase that terminates with an abrupt switch to a warmer phase. Isotopically, the amplitude of a typical DO cycle is about half (up to 75%) of a full glacial-interglacial range (Stuiver & Grootes 2000). Ice-rafted detritus (IRD) in marine sediments show that ice breakouts from Greenland precede abrupt DO warmings (van Kreveld et al. 2000). In the North Atlantic marine sediments, DO cycles have been grouped in combined units (bundles) known as Bond cycles that terminate with IRD horizons known as Heinrich events, from massive ice outbreaks from Labrador (Bond et al. 1993).

Chappell (2002) showed that between 30 and 65 ka BP the Bond cycle bundles of DO cycles correlate with sea-level changes that are recorded in raised coral reefs at Huon Peninsula, Papua New Guinea. The sea-level history derived from precise topographic and stratigraphic data supported by high-precision U-series ages. The simultaneous occurrence of climatically related rapid changes in regions far from the North Atlantic ice fields indicates wide-ranging links in the climate system. Possible mechanisms, many of them reviewed by, for example, van Kreveld et al. (2000), range from luni – solar forcing to the effects of massive iceberg concentrations and meltwater plumes that interrupt the North Atlantic thermohaline circulation (THC) and lead to changes in the other oceans.

Linkages and feedbacks within the climate system range from methane pulses from the oceans (Kennett et al. 2000) to aridity-driven fluctuations of atmospheric dust (Broecker 2000).

Whatever the causes, as summarized by Chappell (2002), ice sheets are involved but possible behaviours range from collapse and surge of unstable sheets to slower cycles of ice growth and decay. The amplitude, rate and timing of the resulting sea-level changes depend on the ice breakout mechanism.

Previously we have shown that between 11 and 45 (^{14}C) ka BP, semi-cycles comparable to the Bond cycle bundles of DO cycles are recorded from terrestrial and marine data from Norway, hosting the western part of the Fennoscandian ice sheet. Each semi-cycle started with a gradual, but relatively fast change to a cold phase and build-up of merging glaciers, which eventually became an ice sheet that deposited tills on a regional scale. Each major cold phase terminated with an abrupt switch to a warmer phase with ice retreat and regional deposition of glaciofluvial sediments (Olsen et al. 2001a, b, c, 2002).

In this paper, we present and discuss the cyclical nature of the distribution of 264 dates from ice-free periods during this age interval. We do this on the basis of statistical treatment using methods including spectral analysis and autocorrelation. Furthermore, we discuss the possible causes of such variations, for example sea-level changes that may have been an important factor for the regional timing of the glacial events, but we also discuss briefly other mechanisms such as the internal cyclicity of ice sheets (Ghil 1988, Cutler et al.1998).

Climatic cycles known as Milankovitch cycles, with periods of c. 20, 40 and 100 ka, are linked to orbital changes (e.g., Imbrie et al. 1984, Ruddiman 2003), but also sub-Milankovitch cycles may be due to external forcing, such as changes in the magnetic field causing changes in the atmospheric ^{14}C-level (e.g., Stuiver & Quay 1980). A cyclicity in the atmospheric ^{14}C-content with duration comparable to the half-life of ^{14}C, i.e. c. 5.7 ka, may possibly exist, but is not thought to be a result of solar forcing only. Variations in oceanic THC, which may lead to a differential transfer of CO_2 between the oceans and the atmosphere, are also thought to cause changes in the ^{14}C-content of the atmosphere. We will also address such issues briefly in the present paper. Recently, the main results of our studies have been presented in a preliminary poster version at the last Nordic Geological Winter meeting in Uppsala (Olsen & Hammer 2004).

Setting

Norway is characterised by a highly irregular mountainous terrain with a densely dissected coastline and deeply incised fjords and valleys (Fig.1), ideal for rapid ice growth and decay. Considering the westerly position of the mountain areas above 900 m a.s.l. in Fennoscandia (lightest areas in Fig.1a), the initial ice growth during the last glaciation must have started in central southern Norway, in the highest mountains along the coast and along the Norwegian-Swedish national border in the north. Conditions favourable for glaciation are enhanced by the short distances to principal moisture sources, which are the North Atlantic and the Norwegian Sea in the west. However, the long coastline and the deep and long fjords may also have functioned in the opposite direction with many 'entry' points for the sea to destabilize an extensive ice-sheet, such as that which existed during the last glacial maximum (Olsen et al. 2001b).

The deep fjords, as well as the long and deep trenches trending parallel to the coast on the adjacent shelf, e.g. the Norwegian Channel – Skagerrak trench, may have functioned as effective calving channels during ice-stream retreat and disintegration. It is likely that the first significant

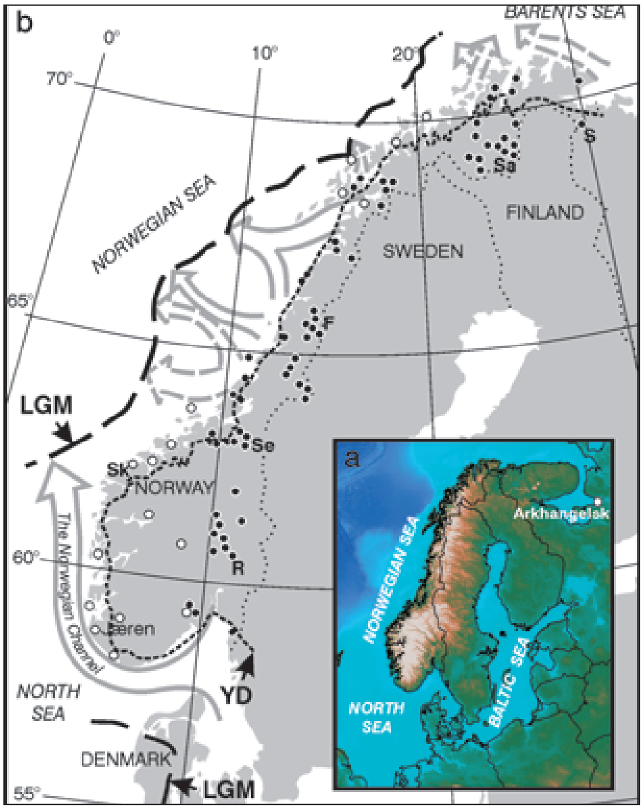

Fig.1: (a) Topography of Fennoscandia and adjacent areas. (b) Stratigraphical sites with dates used in this study (after Olsen et al. 2001a, b, c): • = our own data; ○ = other sources; S= Skjellbekken, Sa= Sargejohka, F= Fiskelauselva, Se=Selbu, Sk= Skjonghelleren, and R= Rokoberget are all sites of major importance for the interpretations of glacial fluctuations during the Middle to Late Weichselian. Positions for LGM (stippled) and YD (dotted line) ice margins and offshore ice streams (broad arrows) are also indicated.

hindrance to rapid ice retreat in the North Sea area would have been the shallower areas at the 'outlet' of the Baltic Sea basin. Considerable ice retreat along the Norwegian coast in some intervals may therefore, although different from the last deglaciation, have occurred without a major contemporary ice retreat in the Baltic Sea region (Fig.1).

Sampling analysis and initial data evaluation

The description of sampling procedures and analyses was published by Olsen et al. (2001a, b, c), from which the most important criteria for randomness and representativity of the samples are found and repeated here. The samples are taken from sediment units representing ice-free conditions during the interval 11-45 ka (^{14}C) BP. The samples are from 75 localities spread over most of Norway (Fig. 1), and they are selected so that all recorded major ice-free events from this interval are represented from most localities. Most samples are taken from fine-grained sediments showing no traces of oxidation or other influences of water circulation. All sampled sediment successions are located above the present local groundwater table. The samples have been air-dried, and generally treated with care to prevent during-and-after-sampling carbon contamination. These precautions include storage in plastic bags, in a refrigerator (+ 4°C) to prevent fungus production, before laboratory dating analysis.

The availability of natural sections, excavations and other sites relevant for sampling may have introduced some sample bias with an influence of some ice-free intervals in some areas, but looking at the whole ensemble of samples this effect is clearly diminished and the randomness of the sampling is achieved.

Radiocarbon dates constitute the majority (88%) of the dates used here, and these were performed at the R.J. Van de Graaff Laboratory at the University of Utrecht (UtC-numbers; AMS ^{14}C dates of sediment samples), the Radiometric Dating Laboratory in Trondheim (T-numbers; conventional radiocarbon dating, mainly of shells), and the T. Svedborg Laboratory, Uppsala University (Ua- and Tua-numbers; AMS ^{14}C dates), all well-established, high-quality dating laboratories. For details and information on the remaining 12% of the dates, see Olsen et al. (2001a, b).

To prevent contamination from carbon from dissolved matter in circulating water / groundwater, the majority of the dates from organics (mainly bulk plant remains) in sediments are from the insoluble (INS) fraction. This fraction comprises organic matter which seems to be almost unaffected by dissolved matter in circulating water, whereas the soluble (SOL) fraction is often very much affected (Olsen et al. 2001a). However, about 1/3 of the dates are from organic-poor sediments, and this introduces a possible significant error which can never be 100% accounted for. This error represents general carbon contamination, at any stage in the sediment history, both before, during and after sampling. Such contamination will obviously much more easily affect a sample with low rather than with high organic content.

The component of this error, possibly introduced during laboratory analysis, is minimised by using more than 0.9 mg C as the amount of material used for each AMS measurement (Olsen et al. 2001a). The error component possibly introduced during sampling and storage before analysis is also accounted for (Olsen et al. (2001a), but the initial error component, which is possibly introduced before sampling, is less straightforward to minimise.

Organic remains in sediments are often a mixture of components from materials of different age, perhaps even representing different ice-free intervals. If the total organic content is small, then a separation of such components may be difficult, or even impossible. Therefore, the age resulting from the dating of such a sample will be an average for the represented components, of which perhaps only one may represent the hosting unit. To diminish this possible error several dates are, in some cases, taken from different positions in the same unit. The youngest ages are then regarded as representatives for the age of the unit. Though sometimes reduced in significance, e.g. by this kind of quality improvements, such possible pre-sampling contamination cannot be fully eliminated as an uncertainty factor for many of the 1/3 of the sample ensemble that has a low organic content. However, since this is not a major problem for most of the samples (more than 2/3), and as the total sampling error is little and, furthermore, as the randomness and representativity of the samples are good (as mentioned above), we think that our data should be well fitted for statistical treatment, including, for example, spectral analysis (Fig. 2, and next chapter).

An initial evaluation of which type of distribution of events in time is represented by our data may be based on previous presentations of the data given by Olsen et al. (2001a, b, c, d). It is clear from these papers that all dates derive from ice-free intervals that are separated by ice-cov-

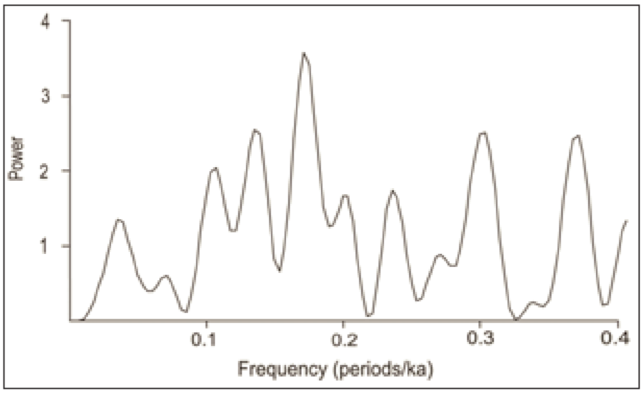

Fig.2: Spectrogram of the distribution of ^{14}C-ages of 264 dates ranging between 11 and 45 ka BP, from non-glacial intervals in Norway, showing a distinct spectral peak for a period of 6000 years (0.17 periods per thousand years). Horizontal axis is frequency (periods per thousand years), vertical axis is power (square of amplitude in arbitrary units), p= 0.05 significance level is at a power of 7.5.

ered intervals of comparable, but at least slightly different lengths. This means that the distribution is not strictly regular, but rather of a semi-regular character. Other common types of distribution, as described e.g. by Swan & Sandilands (1995), are named 'random', 'clustered', 'trend' and 'pattern'. Of these, the type named 'pattern' with several events distributed in groups separated by intervals of comparable lengths, showing most similarities with our data, and may also be described as semi-regular in character. Therefore, we think that our data in general are close enough to uniformity, the fundamental assumption of a time series, to be subjected to statistical analysis.

Statistical methods and results

The time series as given in Figs. 3 and 4 can be investigated with respect to possible periodical components, and any periodicities can be tested against the null hypothesis of an uncorrelated, flat-spectrum, stochastic signal (white noise). It is important to stress that the statistical procedures simply test whether it is likely that the time series *as given* could have been taken from a population of random time series. The tests themselves do not address, nor assume, any level of quality in the data, including dating accuracy. Obviously, it is conceivable that errors, bias or other inaccuracies in the data could produce the observed periodicity, and this would not be detected by the statistical tests given here.

The most common method for detecting periodicity in a time series is spectral analysis, resulting in a spectrogram where 'power' (squared amplitude) is plotted as a function of frequency, i.e. number of cycles per time unit. Strong periodicities will appear as peaks in the spectrum (e.g., Press et al. 1992).

Spectral analysis is here performed to test whether the distribution of dates from 75 Norwegian localities (Fig. 1), with terrestrial and raised marine sediments from the interval 12-50 cal ka BP (11–45 ^{14}C ka BP), is influenced by a climatic variable of sinusoidal character. The dates, of which c. 1/3 are from organic-poor sediments (< 5% loss-on-ignition), are taken from compilations presented by Olsen et al. (2001a, b) and represent mainly ^{14}C-dates of sediments (45%) and shells (37%), but also other materials (speleothems, bones and calcareous concretions) and methods (TL, OSL and U/Th; comprising 12% of the dates) are included (Tables 1-3). For direct comparison of all age estimates, those not based on the radiocarbon method (12%) were corrected to the ^{14}C-yr time-scale using the procedure described by Olsen et al. (2001a), and when referring to the calendar year (cal yr) time-scale in text and illustrations we have converted the ^{14}C-ages to cal years after Kitagawa & van der Plicht (1998), including extrapolation over 45 cal ka BP. We have chosen not to use INTCAL98, and extrapolation over 24 cal ka BP (Stuiver et al. 1998), since that method is based on much fewer data points in the upper part of the time-scale.

Spectral analysis was carried out using the Lomb periodogram method (Press et al. 1992). Prior to analysis, the curves were detrended by subtracting the straight line obtained by linear regression. No single sinusoidal component reaches the $p<0.05$ significance level, although a relatively strong peak is present at a frequency of 0.17 periods per ka for 264 ^{14}C-ages of various samples (sediments, shells and other materials) from different localities (Figs. 1 & 2). This implies a possible effect of a 6000 yr climatic cycle, as

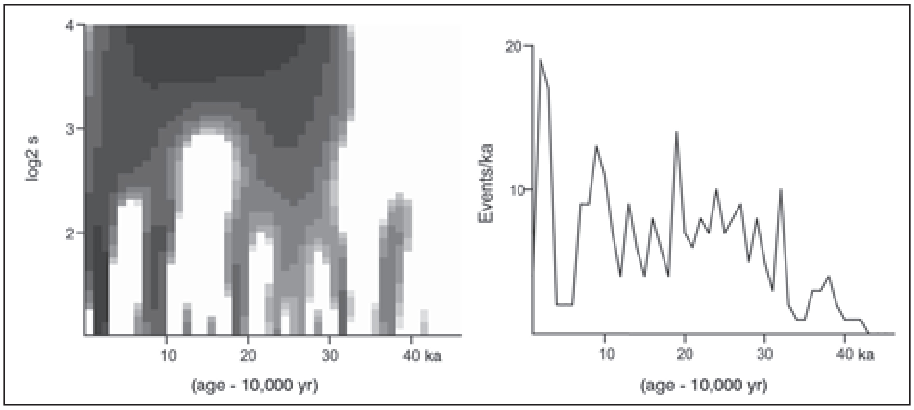

Fig.3: Continuous wavelet scalogram of the distribution of the same dates as in Fig.2, and (to the right) distribution of dates. The vertical axis of the scalogram is in units of the logarithm (base 2) of the scale(s) at which the time series is observed. Signal strength (correlation with the wavelets) is shown in a grey tone. The horizontal axes are in ka and represent a time scale with age – 10,000 yr.

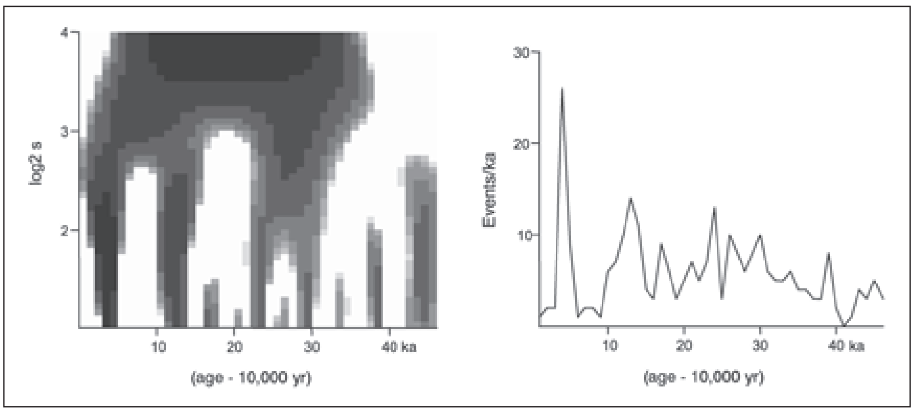

Fig.4: Continuous wavelet scalogram of the distribution of the same dates as in Fig.2, but converted to calendar ages as described by Olsen et al. (2001a); and (to the right) distribution of dates. The horizontal axes are in units of time, as in Fig. 3.

Table 1: Sediment dates, based on ^{14}C and ^{14}C-AMS methods. All ages in yrs BP.

Locality	Lab.no.	Fraction	^{14}C-yr	+/-1 std	cal yr (1)*	+/- 1 std (1)*	cal yr (2)**	+/- 1 std (2)**	Refr.
Komagelva	UtC 1795	INS	16 420	190	19 600	200	19 200	200	1
Komagelva	UtC 3458	INS	14 380	140	17 200	200	16 800	200	1
Leirelva	UtC 1799	INS	17 290	170	20 530	300	19 900	300	1
Leirelva	UtC 1800	SOL	17 110	160	20 350	300	19 800	300	1
Leirelva	UtC 3460	SOL	18 680	170	22 200	300	21 900	300	1
Skjellbekken	UtC 4039	INS	34 000	600	38 800	600	36 000	600	1
Skjellbekken	UtC 4040	INS	25 860	280	30 000	500	29 800	500	1
Kroktåa	UtC 7394	INS	13 950	90	16 750	200	16 550	200	1
Mågelva	UtC 7456	INS	13 890	140	16 680	200	16 350	200	1
Urdalen	UtC 8458	INS	20 470	110	24 200	300	23 900	300	1
Urdalen	UtC 8459	INS	27 580	220	32 500	500	31 250	500	1
Meløy	UtC 8456	INS	17 700	80	21 000	300	20 500	300	1
Kjelddal I	UtC 8457	INS	18 880	100	22 380	300	21 970	300	1
Kjelddal II	UtC 8313	INS	24 858	161	29 000	400	28 250	400	1
Grytåga	UtC 5557	INS	35 400	500	39 300	500	38 100	500	1
Risvasselva	UtC 5558	INS	36 800	600	42 000	600	39 350	600	1
Luktvatnet	UtC 4715	INS	30 600	300	35 200	500	32 650	500	1
Grane, F.	UtC 2215	INS	28 000	500	32 500	500	31 600	500	1
Grane, F.	UtC 2216	INS	19 500	200	23 100	300	23 000	300	1
Grane, F.	UtC 3466	INS	29 400	500	33 900	500	32 200	500	1
Grane, N.	UtC 3467	INS	26 400	400	30 900	500	31 100	500	1
Hattfjelldal	UtC 2212	INS	27 300	600	31 700	600	31 300	600	1
Hattfjelldal	UtC 2213	INS	30 500	600/700	35 400	700	32 650	700	1
Hattfjelldal	UtC 2214	INS	25 700	600	30 000	600	29 800	600	1
Hattfjelldal	UtC 4720	INS	28 060	220	32 500	500	31 600	500	1
Hattfjelldal	UtC 4721	INS	25 370	170	29 500	400	29 800	400	1
Hattfjelldal	UtC 4802	SOL	25 980	240	30 400	500	29 800	500	1
Hattfjelldal	UtC 4804	SOL	25 780	240	30 000	500	29 800	500	1
Hattfjelldal	UtC 4807	INS	26 720	280	31 150	500	31 200	500	1
Hattfjelldal	UtC 4809	INS	23 500	240	27 750	400	26 400	400	1
Slettåsen	UtC 4722	INS	34 900	400	39 200	500	36 700	500	1
Røssvatnet	UtC 3468	INS	31 000	500	35 750	500	33 100	500	1
Røssvatnet	UtC 3469	INS	29 700	500	34 300	500	32 200	500	1
Langstr.bak.	UtC 5974	INS	18 700	500	22 300	500	21 900	500	1
Øyvatnet	UtC 4718	INS	22 330	150	26 500	400	25 350	400	1
Øyvatnet	UtC 4800	Hexane	19 340	150	23 000	300	22 200	300	1
Gartland	UtC 4719	INS	28 000	200	32 500	500	31 600	500	1
Gartland	UtC 4871	SOL	16 250	190	19 400	200	19 100	200	1
Namsen	UtC 4811	Hexane	16 110	120	19 180	200	19 000	200	1
Namsen	UtC 4812	INS	18 580	140	22 150	300	21 850	300	1
Namsen	UtC 4813	INS	18 020	170	21 400	300	21 000	300	1
Namskogan	UtC 3465	INS	28 700	400	33 250	500	32 000	500	1
Ø.Tverråga	UtC 3464	INS	17 830	190	21 000	300	20 500	300	1
Nordli	UtC 1380	INS	41 000	3000/2000	47 830	3000	43 100	3000	1
Blåfjellelva II	UtC 5565	INS	19 710	110	23 300	300	23 400	300	1
Blåfjellelva II	UtC 5566	INS	20 040	100	23 700	300	23 700	300	1
Blåfjellelva I	UtC 3463	INS	22 220	240	26 250	400	25 200	400	1
Humm.,Swe.	UtC 4814	INS	22 070	170	26 000	400	25 100	400	1
Sitter	UtC 2103	INS	30 200	400	35 300	500	32 600	500	1
Sitter	UtC 4717	INS	21 150	130	25 000	400	24 400	400	1
Sitter	UtC 4799	SOL	12 480	70	15 000	100	15 000	100	1
Myrvang	UtC 4716	INS	16 770	190	20 200	300	19 400	300	1
Reinåa	UtC 5549	INS	28 700	300	33 250	500	32 000	500	1
Reinåa	UtC 5550	INS	16 850	90	20 300	300	19 850	300	1
Reinåa	UtC 5551	INS	19 880	160	23 600	300	23 600	300	1
Reinåa	UtC 5552	INS	31 600	400	36 250	500	33 750	500	1
Reinåa	UtC 5553	INS	29 280	260	33 900	500	32 200	500	1
Reinåa	UtC 5554	INS	30 900	300	35 750	500	33 100	500	1
Stærneset	UtC 5555	INS	18 820	110	22 380	300	21 970	300	1
Stærneset	UtC 5556	INS	25 240	180	29 500	400	29 800	400	1
Grytdal	UtC 4714	INS	38 500	700	44 555	700	41 000	700	1
Grytdal	UtC 5559	INS	39 500	800	46 105	800	41 800	800	1
Grytdal	UtC 5560	INS	37 200	600	43 460	600	39 800	600	1
Grytdal	UtC 5561	INS	41 800	1000/1100	48 750	1100	44 100	1100	1
Grytdal	UtC 5562	INS	23 700	200	27 800	400	26 500	400	1
Grytdal	UtC 5563	INS	25 300	260	29 500	400	29 800	400	1
Grytdal	UtC 5564	INS	28 400	300	33 000	500	31 800	500	1
Grytdal	UtC 6040	INS	18 970	150	22 400	300	22 000	300	1
Flora	UtC 5977	INS	17 800	400	21 000	400	20 500	400	1
Flora	UtC 5978	INS	15 920	260	19 000	260	18 800	260	1
Flora	UtC 5979	INS	17 800	400	21 000	400	20 500	400	1
Flora	UtC 5981	INS	16 700	220	20 200	300	19 400	300	1
Flora	UtC 5982	INS	15 620	200	18 600	200	18 400	200	1
Flora	UtC 5984	INS	19 600	280	23 100	280	23 000	280	1
Flora	UtC 6042	INS	19 050	120	22 450	300	22 050	300	1
Flora	UtC 5985	INS	18 000	400	21 400	400	21 000	400	1
Kollsete	UtC 6046	INS	22 490	180	26 700	400	25 500	400	1
Skjeberg	UtC 1801	INS	19 480	200	23 100	300	23 000	300	1
Skjeberg	UtC 1802	SOL	16 770	190	20 200	300	19 400	300	1
Herlandsdal.	UtC 4728	INS	32 000	300	36 800	500	33 800	500	1
Herlandsdal.	UtC 4729	INS	28 300	240	33 000	500	31 800	500	1
Herlandsdal.	UtC 6045	INS	23 250	170	27 400	400	26 200	400	1
Passebekk	UtC 6044	INS	28 600	300	33 200	500	32 000	500	1
Passebekk	UtC 5987	INS	21 000	400	24 800	400	24 200	400	1
Rokoberget	UtC 1962	INS	47 000	4000/3000	54 730	4000	49 600	4000	1
Rokoberget	UtC 1963	INS	33 800	800/700	38 800	800	35 500	800	1
Dokka, K.	UtC 3462	INS	26 800	400	31 200	500	31 250	500	1
Dokka, K.	UtC 2218	INS	18 900	200	22 400	300	22 000	300	1
Mesna, Lh.	UtC 6041	INS	16 030	100	19 150	200	18 900	200	1
Mesna, Lh.	UtC 1964	INS	36 100	900/800	41 895	900	38 900	900	1
Mesna, Lh.	UtC 2217	INS	31 500	700	36 100	700	33 600	700	1
Stampesletta	TUa ***	INS	16 000	***	19 150	200	18 900	200	1
Stampesletta	UtC 1965	INS	32 300	500	36 800	500	33 800	500	1
Gråbekken	UtC 4723	CO3	41 300	900/1000	48 000	1000	44 000	1000	1
Folldal	UtC 4724	CO4	36 300	500/600	41 900	600	38 900	600	1
Folldal	UtC 4709	INS	26 260	220	30 700	500	30 900	500	1
Folldal	UtC 4710	SOL	23 260	160	27 400	400	26 200	400	1
Surna	UtC 10110	INS	19 090	100	22 450	300	22 050	300	0
Bogneset	UtC 10109	INS	20 880	130	24 600	300	24 150	300	0

*: Calendar years; calibrated age after age model 1: after INTCAL98, and extrapolation for ages higher than 24,000 cal yr BP (Stuiver et al. 1998).
**: Calendar years; calibrated age after age model 2: after Kitagawa & van der Plicht (1998), and extrapolation over 45,000 cal BP.
***: Numbers not available; preliminary report (S. Gulliksen, pers. comm. 1995).
Refr. 0, this work; refr. 1, Olsen et al. 2001a.

also illustrated in wavelet transforms for ^{14}C-ages and calendar scale calibrated ages (Figs. 3 & 4).

Wavelet analysis (Percival & Walden 2000) allows the study of a time series at several different scales, and can highlight non-stationary periodicities. The result of the analysis is presented in a scalogram, which is a diagram with time along the horizontal axis and the logarithm of scale along the vertical axis. Strength of the signal at any particular time and scale, that is, degree of correlation with the scaled and translated wavelets, is shown using a grey-scale. Long-term (large-scale) features can then be read along the top of the diagram, while short-term (small-scale) details can be read along the bottom.

For description of autocorrelation, the third statistical method used here, we refer to Davis (1986). Autocorrelation proceeds by correlating the time series with a copy positioned at progressively increasing time delays (lag times). The correlation coefficient as a function of lag time will show a distinct peak at lag times corresponding to periodicities in the signal, also for non-sinusoidal components.

We have used this method to test whether the variations may be of a narrow spike character rather than sinusoidal, but it is difficult to find a statistical method that is really good to test the significance of such variations. The significance may therefore be better than we have found. The time series was detrended, as described above, also prior to wavelet analysis and autocorrelation.

The results from the autocorrelation analysis indicate that a narrow spike/ abrupt pulse climatic cycle of 6000 yr length may well be present in the data. This cycle is significant at $p<0.05$, with respect to the null hypothesis of uncorrelated white noise, as shown in Fig. 5.

At higher significance levels the distribution of dates follows a less distinct cyclical pattern, and are in these cases not significant as cycles, but may be better described as semi-cycles. This is probably a result of the inhomogeneity of the dates, materials and environments that are represented. The high vulnerability for contamination for 1/3 of the samples (those with low organic carbon content) may also have resulted in local variations.

Comparison with Greenland ice-core data

The Greenland ice-core stratigraphy is primarily based on electric conductivity, various chemical data, counting of visible annual layers and $\delta^{18}O$ curves. Distinct fluctuations seen in time scales of several years to many decades, observed in most detailed isotope records, do not necessarily have climatic significance (e.g., Grootes et al. 1990). There are a number of problems connected with ice cores, such as representativity as archives for atmospheric conditions, disturbances and contamination of chemical species during drilling, transportation, storage and analy-

Table 2: Shell dates, based on ^{14}C and ^{14}C-AMS methods. All ages in yrs BP

Locality	Lab.no.	Material	^{14}C-yr	+/- 1 std	cal yr (1)*	+/- 1 std (1)*	cal yr (2)**	+/- 1 std (2)**	Refr.
Kroktåa	UtC 7350	shell	12 430	80	14 360	400	14 600	350	1
Storelva	UtC 7345	shell	41 660	1500	48 500	1500	44 100	1500	1
Mågelva	UtC 7346	shell	11 270	80	13 170	100	12 970	100	1
Mågelva	UtC 7347	shell	11 680	70	13 400	400	13 250	400	1
Mågelva	UtC 7348	shell	11 060	70	13 065	100	12 900	100	1
Mågelva	UtC 7349	shell	45 560	2400	53 000	2400	48 100	2400	1
Meløya	UtC 8310	shell	38 200	700	44 000	700	40 840	700	1
Skavika	T-10798	shell	11 865	60	13 830	100	13 550	100	1
Stamnes	T-10541	shell	12 420	105	14 350	105	14 600	400	1
Bogneset I	T-10540	shell	32 100	2600	36 900	2600	33 900	2600	1
Bogneset I	TUa-947	shell	40 025	965	46 655	1000	42 200	1000	1
Bogneset I	TUa-1239	shell	35 940	1455	41 100	1500	38 650	1500	1
Bogneset I	TUa-1240	shell	28 355	430	33 000	500	31 800	500	1
Bogneset I	TUa-1241	shell	38 090	1675	43 900	1675	40 600	1675	1
Bogneset II	T-11784	shell	11 165	105	13 150	105	12 950	105	1
Storvika	UtC 4727	shell	11 110	80	13 100	100	12 900	100	1
Skogreina	TUa-743	shell	38 545	835	44 555	835	41 000	835	1
Skogreina	TUa-946	shell	37 730	735	43 730	735	40 300	735	1
Skogreina	TUa-1092	shell	38 060	710	43 900	710	40 600	710	1
Stigen	UtC 8314	shell	12 200	60	13 970	100	14 300	400	1
Åsmoen	TUa-567	shell	28 355	235	33 000	500	31 800	500	1
Åsmoen	TUa-744	shell	12 520	85	14 880	390	14 600	400	1
Mosvollelva	TUa-1094	shell	29 075	370	33 575	400	32 100	400	1
Djupvika	T-10543	shell	10 430	185	12 465	185	12 225	275	1
Vargvika	T-10797	shell	12 450	195	14 380	195	14 600	400	1
Ytresjøen	UtC 8315	shell	28 720	240	33 250	500	32 000	500	1
Ytresjøen	UtC 8316	shell	35 500	600	39 400	600	38 250	600	1
Vassdal f.q.	TUa-944	shell	35 280	575	39 100	575	37 900	575	1
Vassdal	T-10796	shell	30 610	3950	35 550	3950	32 800	3950	1
Holmåga	UtC 8308	shell	9 059	39	10 230	100	10 250	100	1
Sandvika	UtC 8309	shell	12 600	60	14 900	400	14 680	400	1
Neverdalsvat.	T-11785	shell	12 520	205	14 880	390	14 600	400	1
Nattmålsåga	T-12567	shell	11 975	155	13 950	155	13 610	155	1
Fonndalen	UtC 5465	shell	11 990	60	13 950	100	13 800	175	1
Aspåsen	TUa-1386	shell	36 455	530	41 950	530	39 125	530	1
Oldra	TUa-745	shell	32 510	395	37 100	500	34 050	500	1
Oldra	TUa-1385	shell	33 040	315	37 750	500	34 600	500	1
Oldra II	TUa-1387	shell	33 975	515	38 800	515	35 500	515	1
Kjelddal I	UtC 8311	shell	35 800	600	40 900	600	38 500	600	1
Kjelddal II	UtC 8312	shell	33 700	400	38 650	500	35 350	500	1
Geitvågen	TUa-945	shell	11 140	80	13 130	100	12 935	100	1
Best.m.enga	TUa-1095	shell	11 560	90	13 200	100	13 100	100	1
Hestbakken	UtC 5412	shell	11 770	60	13 550	100	13 400	100	1
Sandjorda	UtC 5413	shell	10 150	70	11 800	100	11 570	250	1
Grytåga	UtC 5463	shell	41 460	900	48 400	900	44 000	900	1
Holstad	TUa-943	shell	10 245	80	11 925	125	11 690	150	1
Finneid g. pit	TUa-1097	shell	10 585	80	12 725	100	12 300	100	1
Hundkjerka	TUa-1093	shell	46 340	1620	53 800	1620	49 000	1620	1
Langstr.bak.	T-12564	shell	36 950	2700	42 700	2700	40 000	2700	1
Sitter	UtC 4726	shell	12 490	70	14 360	400	14 600	400	1
Myrvang	UtC 5414	shell	12 070	60	13 960	100	14 100	100	1
Osen	T-11961	shell	11 615	95	13 300	400	13 150	400	1
Osen	T-11963	shell	12 000	125	13 950	125	14 100	125	1
Osen	TUa-1238	shell	39 140	2425	45 200	2425	41 500	2425	1
Reveggheia	T-11960	shell	12 035	230	13 950	230	14 100	230	1
Gjevika	T-11962	shell	12 325	215	14 480	215	14 400	400	1
Follafoss	TUa-1260	shell	46 905	4020	54 500	4020	49 500	4020	1
Follafoss	TUa-1261	shell	47 565	4680	55 380	4680	50 165	4680	1
Kvitnes	TUa-3622	shell	39 495	870	46 105	870	41 800	870	0
Løksebotn I	TUa-3623	shell	47 815	2305/1790	55 660	2305	50 415	2305	0
Leirhola	TUa-3624	shell	44 755	1745/1435	52 150	1745	47 355	1745	0
Nyheim	T-15733	shell	11 425	115	13 430	115	13 064	140	0
Skjervøy	T-15735	shell	11 120	95	13 100	100	12 900	100	0
Brøstadelva	T-15721	shell	11 125	130	13 100	130	12 900	130	0
Nonsfjellet	T-15722	shell	11 465	185	13 470	185	13 100	185	0
Raudskjer	TUa-3540	shell	42 260	1165/1020	49 200	1165	45 000	1165	0
Risøya	TUa-3541	shell	11 135	75	13 100	100	12 900	100	0
Løksebotn II	TUa-3542	shell	11 685	75	13 300	100	13 150	100	0
Kjølvik	TUa-3539	shell	12 260	105	14 000	105	14 200	105	0
Kjølvik	T-15723	shell	12 160	145	13 960	145	14 020	145	0
Skulsfjord	T-16022	shell	12 165	185	13 960	185	14 025	185	0
Dåfjorden	T-16023	shell	11 090	80	13 090	100	12 900	100	0
Hessfjorden	T-16024	shell	12 080	155	13 960	155	14 100	155	0
Kjelddal II	TUa-3625	shell	40 300	870	47 000	870	42 400	870	0
Leirhola I	TUa-3626	shell	48 635	2595/1960	56 600	2600	51 200	2600	0
Nesavatnet	TUa-2526	shell	36 815	590	42 000	590	39 350	590	0
Skjenaldelva	TUa-2996	forams	33 620	470	38 400	500	35 100	500	0
Skjenaldelva	TUa-2997	forams	34 155	620	39 000	620	36 000	620	0
Kjelddal I	UtC 10100	forams	34 460	400	39 900	500	36 700	500	0
Løksebotn I	UtC 10103	shell	44 560	2000	52 500	2000	47 600	2000	0

Table 3: Various dates and methods (after Olsen et al. 2001a). All ages in yrs BP

Dating method	Locality	Lab.no.	Material	14C-yr	+/- 1 std	cal yr (1)*	+/- 1 std (1)*	cal yr (2)**	+/- 1 std (2)**	Refr.
OSL	Komagelva	R-933801	sand, gl.fl.	14500	2000	17 000	2000	16 600	2000	1,2
OSL	Leirelva	R-943801a	sa-silt, gl.lac.	22000	2500	26 000	3000	25 000	3000	1,2
TL	Leirelva	R-943801b	sa-silt, gl.lac.	22000	2500	26 000	3000	25 000	3000	1,2
14C-AMS	Sargejohka	UtC-1392	gy-silt; INS"	37100	1600	43 200	1600	39 700	1600	1,2,3
TL	Kautokeino	R-823820a	sand, gl.fl.	33000	3500	37 000	5000	34 750	5000	1,2,3
TL	Kautokeino	R-823820b	sand, gl.fl.	37000	4000	41 000	5000	38 900	5000	1,2,3
14C	Lauksundet	T-***	shell	27000	***	31 200	500	31 300	500	1,4
14C	Leirhola	T-***	shell	30000	***	35 000	500	32 300	500	1,4
14C	Kvalsundet	T-2377	shell	40600	2100/1700	47 000	2100	43 000	2100	1,5
14C	Slettaelva	T-***	shell	41900	2800/2100	48 500	2800	44 500	2800	1,5
14C-AMS	Bleik	Ua-1043	shell	17940	245	21 140	300	20 750	300	1,6
"AAR; alle/Ile"	Bleik	BAL 1780	shell	22000	***	26 000	400	25 000	400	1,6
"AAR; alle/Ile"	Bleik	BAL 1785	forams	22000	***	26 000	400	25 000	400	1,6
14C	Endletvatnet	T-1775A	algal si.,SOL	18100	800	21 400	800	21 000	800	1,7
14C	Endletvatnet	T-1775B	algal si.,INS	19100	270	22 500	300	22 100	300	1,7
14C	Æråsvatnet	T-5581	macro algae	17800	230	21 000	300	20 500	300	1,8
14C	Æråsvatnet	T-4791A	algal si.,SOL	17910	820	21 100	820	20 700	820	1,8
14C	Æråsvatnet	T-4791B	algal si.,INS	18950	280	22 480	300	22 000	300	1,8
14C	Æråsvatnet	T-5278B	algal si.,INS	18950	1090	22 480	1090	22 000	1090	1,8
14C	Æråsvatnet	T-4793A	algal si.,SOL	19100	670	22 500	670	22 100	670	1,8
14C	Æråsvatnet	T-4793B	algal si.,INS	20780	540	24 450	540	24 000	540	1,8
14C	Øv.Æråsvat.	T-8559A	gyttja,SOL	18820	200	22 380	300	21 970	300	1,9
14C	Øv.Æråsvat.	T-8558A	gyttja,SOL	19650	180	23 200	300	23 100	300	1,9
14C	Øv.Æråsvat.	T-8029A	si-gy,gl.lac.	21800	410	25 700	410	24 800	410	1,9
14C	Øv.Æråsvat.	T-8029B	si-gy,gl.lac.	21520	150	25 400	400	24 500	400	1,9
14C	Bøstranda	T-3942	shell	39150	900/800	45 600	900	41 500	900	1,10
14C-AMS	Trenyken	Ua-2016	shell	33560	1150	38 300	1150	35 050	1150	1,6
14C	Kj.vik, cave	TUa-436	bone	20110	250	23 820	300	23 700	300	1,11
14C	Kj.vik, cave	TUa-488	bone	20210	130	23 970	300	23 800	300	1,11
14C	Kj.vik, cave	TUa-485	bone	22500	260	26 500	400	25 500	400	1,11
14C	Kj.vik, cave	TUa-489	bone	31160	300	35 800	500	33 260	500	1,11
14C	Kj.vik, cave	TUa-487	bone	39365	640	45 850	600	41 750	600	1,11
14C	Kj.vik, cave	TUa-346	bone	41120	1480/1250	48 000	1480	43 400	1480	1,11
U/Th	Kj.vik, cave	ULB 846	calc.concr.	17000	***	20 000	600	19 570	600	1,11
U/Th	Kj.vik, cave	ULB 863	calc.concr.	36000	***	40 000	600	37 150	600	1,11
14C	Rana, cave	T-12093	calc.concr.	23345	145	27 500	400	26 200	400	1
14C	Rana, cave	T-12092	calc.concr.	29360	255	33 900	500	32 200	500	1
14C	Rana, cave	T-12089	calc.concr.	31910	335	36 600	500	33 700	500	1
14C	Rana, cave	T-12090	calc.concr.	32470	325	37 000	500	33 900	500	1
14C	Rana, cave	T-12091	calc.concr.	46560	2700/2000	54 000	2700	49 200	2700	1
14C	Vassdal	T-2670	shell	34330	1630/1410	39 200	1630	36 200	1630	1,12
14C	Svellingen	T-4004	shell	42400	1280/1110	49 300	1280	45 000	1280	1,13
14C	Ertvågøya	T-8071	shell	41500	3130/2240	48 400	3130	44 000	3130	1,14
14C	Kortgarden	T-7281	shell	26940	670	31 500	670	31 400	670	1,15
14C	Eidsvik	T-2657	shell	35700	1100	40 200	1100	38 450	1100	1,16
14C	Gaml.veten	T-***	soil,bulk org.	20000	***	23 700	300	23 600	300	1,17
14C	Skjonghell.	T-5156	bone	29600	800	34 150	800	32 500	800	1,18
14C	Skjonghell.	T-5593	bone	32800	800	36 600	800	34 500	800	1,18
14C	Skjonghell.	T-***	bone	28900	***	33 500	500	32 350	500	1,19
14C	Skjonghell.	T-***	bone	34400	***	39 300	500	36 300	500	1,19
U-series	Skjonghell.	el 83044	speleothem	25900	1800	29 900	1800	29 800	1800	1,18
U-series	Skjonghell.	el 83142	speleothem	23900	1200	27 900	1200	26 800	1200	1,18
U-series	Skjonghell.	el 83221	speleothem	28000	2000	32 000	2000	31 600	2000	1,18
U-series	Skjonghell.	el 83307A	speleothem	51700	4000	55 700	4000	50 400	4000	1,18
14C-AMS	Hamnsundh.	TUa-806 I	bone	24387	960	28 500	960	27 335	960	1,20
14C-AMS	Hamnsundh.	TUa-806	bone	24555	675	28 700	675	27 700	675	1,20
14C-AMS	Hamnsundh.	TUa-***	bone	27580	***	32 500	500	31 300	500	1,20
14C-AMS	Hamnsundh.	TUa-***	bone	31045	***	35 750	500	33 150	500	1,20
14C-AMS	Hamnsundh.	TUa-***	bone	29745	***	34 350	500	32 250	500	1,20
14C-AMS	Hamnsundh.	TUa-***	bone	31905	***	36 600	500	33 700	500	1,20
14C	Kollsete	T-13211	gyttja,SOL	43800	3700/2500	51 050	3700	46 400	3700	1,21
14C-AMS	Elgane	TUa-***	forams	34820	1165/1020	39 100	1165	36 650	1165	1,22
14C-AMS	Elgane	TUa-***	forams	33480	1520/1280	38 150	1520	34 950	1520	1,22
14C	Foss-Eikela.	T-3423B	shell	31330	700/640	35 900	700	33 400	700	1,23
14C	Oppstad	T-922	shell	41300	6200/3500	48 000	6200	44 000	6200	1,23
14C	Oppstad	T-3422B	shell	38600	1600/1300	44 700	1600	41 150	1600	1,24
14C	Vatnedalen	T-2380	pal.sol,SOL	35850	1180/1040	40 900	1180	38 550	1180	1,25
14C-AMS	Rokoberget	UtC-1963	si,glm,INS	33800	800/700	38 800	800	35 500	800	1,26
14C-AMS	Rokoberget	UtC-1962	cl-si,glm,INS	47000	4000/3000	54 730	4000	49 600	4000	1,26
14C	Sæter, S.Ål	PMO72842a	bone	45400	1500/1200	52 600	1500	48 000	1500	1,27
U/Th	Sæter, S.Ål	PMO72842b	bone	38400	500	42 400	600	40 100	600	1,28
U/Th	Sæter, S.Ål	PMO72842c	bone	48300	900	52 300	900	47 550	900	1,28
U/Th	Sæter, S.Ål	PMO72842d	bone	49700	900	53 900	900	48 860	900	1,28
TL	Sorperoa	R-903301	sand,aeolian	33400	3000	37 400	4000	34 750	4000	1,29
TL	Sorperoa	R-***	sand,aeolian	35300	3000	39 300	4000	36 400	4000	1,29
TL	Sorperoa	R-***	sand,aeolian	36000	4000	40 000	5000	37 800	5000	1,29
TL	Sorperoa	R-***	sand,aeolian	36000	6000	40 000	7000	37 800	7000	1,29
TL	Fåvang	R-897005	sand,gl.fl.	28000	3000	32 000	3000	31 300	3000	1,30
TL	Fåvang	R-897006	sand,gl.fl.	50000	4000	54 000	5000	48 940	5000	1,30
U-series	Fåvang	PMO72843	bone	41300	3000	45 300	2900	41 380	2900	1,28
TL	Haugalia	R-897010	sand,gl.fl.	38000	4000	42 000	4000	39 350	4000	1,30
14C	Gråbekken	T-3556A	gy-sa, SOL	37330	640/590	43 600	640	39 950	640	1,31
14C	Gråbekken	T-3556B	gy-sa, INS	32520	650/590	37 100	650	34 050	650	1,31
14C-AMS	Foss-Eikela.		forams	24210	1880/1520	28 300	1880	27 150	1880	1,32
14C-AMS	Ø-Jotunh.	***	silt, bulk org.	26000	***	30 350	500	30 400	500	1,33

*: Calendar years; given ages for OSL, TL, U/Th and U-series dates, transferred to 14C-ages as described by Olsen et al. 2001a.
** : Calendar years; calibrated age after age model 2 (modified from Kitagawa & van der Plicht 1998).
** : Numbers not available (various sources of information).
Refr. 1, Olsen et al. 2001a; 2, Olsen et al. 1996; 3, Olsen 1988; 4, Andreassen et al. 1985; 5, Vorren et al. 1988; 6, Møller et al. 1992; 7, K.D.Vorren 1978; 8, Vorren et al. 1988; 9, Alm 1993; 10, Rasmussen 1984; 11, Nese & Lauritzen 1996; 12, Rasmussen 1981; 13, Aarseth 1990; 14, Follestad 1992; 15, Follestad 1990; 16, Mangerud et al. 1981; 17, J. Mangerud, pers.comm. 1981; 18, Larsen et al. 1987; 19, Valen et al. 1995; 20, Valen et al. 1996; 21, Aa & Sønstegaard 1997; 22, Janocko et al. 1998; 23, Andersen et al. 1991; 24, Andersen et al. 1987; 25, Blystad 1981; 26, Rokoengen et al. 1993; 27, Heintz 1974; 28, Idland 1992; 29, Bergersen et al. 1991; 30, Myklebust 1992; 31, Thoresen & Bergersen 1983; 32, Raunholm et al. 2002; 33, S. Sandvold, pers.comm. 1997. For references 2-31, see Olsen et al. 2001a.

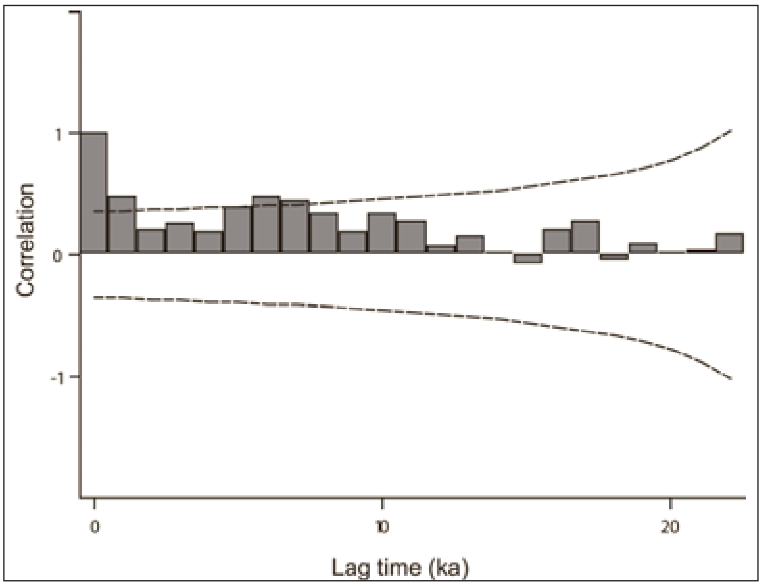

Fig.5: Autocorrelogram of the distribution of the same dates as in Fig.2. Stippled lines indicate 95% confidence interval. A lag time (cycle) of c. 6 ka is significant at p= 0.05, although the multiples occurring at 12 and 18 ka are not very distinct.

sis, etc. (e.g., Jaworowski et al. 1993). However, since paleomagnetic excursions, such as Laschamp and Mono Lake (Lake Mungo), which are independently dated in several parts of the world, were recognised from concentration and flux of ^{36}Cl at the expected places in the GRIP ice core (Wagner et al. 2000), all these problems concerning the chronology and overall $\delta^{18}O$ fluctuations of the ice cores must be regarded as generally small, at least for the last 50 ka. The Greenland ice-core chronology and stratigraphy is therefore, at present, the best available for us to compare our data with.

The resolution for the GRIP ice-core data is 50 yr and for the GISP2 data 60 yr back to 60 ka BP and 50 yr otherwise. The GRIP chronology is based on ice-flow models prior to 11,500 yr BP, whereas the GISP2 chronology is based on counting of annual layers back to 37.9 ka and on tuning to the SPECMAP chronology further back in time (Johnsen et al. 2001). Visual examination of the $\delta^{18}O$-curves, as well as calculations based on running means from the GRIP and GISP2 data sets reduced to a much lower resolution, e.g. 500 yr, transform (some of) the rapid semi-cyclic fluctuations (DO events) to similar, but broader trends in longer intervals (Table 4). The lengths of these intervals back to 90 ka BP vary (range 3-10 ka), but have mean values at c. 6 ka for both ice cores. They must also be climatic signatures since they are based on the same data, although in a more generalised form than for the DO cycles. We have previously compared and found similar trends in climatic fluctuations represented by the major Greenland interstadials (GIS 1, 2, 3-4, 7, 8, 11 and 12) and the ice retreats in the Norwegian glacial record (< 45 ka BP; Olsen et al. 2001b). To present the calculated data here (Table 1) is therefore simply to put numbers to the visual analysis of the trends of the Greenland $\delta^{18}O$-data, as shown before, and to extend this back in time. Although it appears that the lowermost parts (10%) of the GISP2 and GRIP ice cores must have been subjected to flow and folds, and therefore cannot be regarded as reliable with respect to stratigraphic data (Boulton 1993, Grootes et al. 1993), this does not change the results we refer to in Table 4.

The described 6 ka-cycles represented in the Greenland ice-core data are in the same size category as 'our' 6 ka-cycles from the Norwegian (glacial) sediment record. Therefore, the above-mentioned robust matching in time suggests that there may be a one-to-one correlation between the main trends of the Greenland ice-core data and the glacial fluctuations in Norway, at least back to 45 ka BP. This is an intriguing hypothesis, but the chronology of our data is far from being precise enough to accurately show such a relationship. In addition, although there are apparently similar trends in climatic responses, the triggering factors for glacial fluctuations may have been different for the Greenland and the Fennoscandian ice sheets, as exemplified by the present situation (Greenland: big ice sheet; Fennos-candia: no ice sheet, but numerous small ice caps).

Table 4: Major Greenland interstadials (GIS)*, their ages and age differences; $\delta^{18}O$ > -38 per mil.

	GRIP ice-core data		GISP2 ice-core data		Mean age difference	
GIS no.	Age (ka BP)	Age difference (ka)	Age (ka BP)	Age difference (ka)	between major GIS intervals (in ka)	
	9		9.5			
1	14.5	5.5	14.5	5.0	GRIP data:	5.8
2	22.5	8.0	23.5	9.0		Range: 3 - 8.5
3-4	28	5.5	28.5	5.0	GISP2 data:	5.7
5-7	35	7.0	33.5	5.0		Range: 3 - 10.5
8	38	3.0	38	4.5	Both data sets,	
11	43.5	5.5	42.5	4.5	approximate mean	
12	47.5	4.0	45.5	3.0	age difference:	6
14	55	7.5	52	6.5	… and range:	3-10
17	60	5.0	58	6.0		
18	64.5	4.5	62	4.0		
19	73	8.5	68.5	6.5		
20	77	4.0	73	4.5		
21	85	8.0	83.5	10.5		
22	90	5.0	89.5	6.0		

*) Based on GRIP ss09sea and GISP2 Summit ice core data (Johnsen et al. 2001).

Discussion

Since the first ice-core data from the summit area of Greenland were published (e.g., Johnsen et al. 1992, Dansgaard et al. 1993), many other proxy climatic archives from both marine and terrestrial environments have been recorded and correlated with, and show similar cyclicity as the $\delta^{18}O$-curve from Greenland. The lot of these, including those mentioned in the introduction, represent a variety of materials, environments and regions of the world. The Bond cycle bundles of DO cycles, which are recorded in the North Atlantic region, including our terrestrial data from Norway, and the corresponding sea-level changes from Papua New Guinea (see the introduction), strongly suggest a global climatic link between these c. 6 ka (5–7 ka) cycles. The remaining part of the discussion will therefore be focused on which causes are the most likely triggers of these millennial-scale climatic cycles.

The DO events were supposedly triggered by large ice outbreaks from northern Canada and along the margins of Greenland, which resulted in strong variations in the oceanic THC that produced the DO climatic cycles (Rahmstorf 1994, Broecker 1998, van Kreveld et al. 2000). These events dominated only during the cold marine isotope stages, which were characterised by a low global sea level (Schulz et al. 1999), but also with high, local, glacial isostatically determined sea levels. Consequently, the DO cycles, which are not shown to exist during the Holocene, must have had reduced importance for the climate during this interval with its high global sea level, and at a time when ice breakouts are unlikely to have occurred on a large scale along the margins of Eastern and Northern Greenland.

Variations in cosmogenic ^{14}C and ^{10}Be isotopes are supposed to result from solar activity or 'solar forcing' (Beer et al. 2000, 2002). However, only the ^{10}Be flux is widely accepted as a distinct signal of variation in solar activity. In contrast, changes in the atmospheric ^{14}C may result from variations in the oceanic THC, as mentioned before (Beer et al. 2002). Bond et al. (2001) found a relatively close correlation between the climatic variations recorded from marine sediment cores from the North Atlantic Ocean and proxy data for solar activity (^{10}Be from ice cores and ^{14}C from tree-rings). Low solar activity is associated with reduced strength of the magnetic field and therefore increased production of cosmogenic nuclides and is believed to induce climatic deterioration (Stuiver et al. 1995, Grootes & Stuiver 1997), perhaps of the kind that occurred c. 2500 years ago when many small glaciers were produced or increased in size in Norway (e.g., Larsen et al. 2003). Data presented by Bond et al. (2001) indicate that there were eight cold phases, 1000-2000 years apart from each other, during the Holocene, and one of these was that around 8200 years BP, which is also shown to have occurred in several places in Norway (e.g., Nesje et al. 2001, Bjune et al. 2003). However, the prime cause of the brief cold event about 8200 years ago is not considered to have been reduced solar activity, but rather a climatic response to the abrupt catastrophic release of freshwater c. 8450 years BP from the bursting of a huge ice-dammed lake (Lake Agassiz) that had developed in North America along the southern margins of the melting Laurentide ice sheet (Barber et al. 1999).

Most records of climatic variations from the Holocene in different parts of the world indicate a strong correspondence with the 1-2 ka-long, quasi-cyclical variations of the solar activity (e.g., Grønås 2003). Climatic variations from the Antarctic, however, appear to vary in opposite phase with the variations in the north (Dahl-Jensen et al. 1999).

The 6 ka climatic cycle that we have recorded from western Fennoscandia (Norway) for the interval 12-50 (cal) ka BP, and the possible corresponding cycles represented by the Heinrich events in the North Atlantic (Heinrich 1988, Broecker et al. 1992) and the sea-level variations recorded from Papua New Guinea for the interval 30 to 65 ka ago (Chappell 2002), may have been influenced by a set of trigger mechanisms that all are constrained to glaciations. For example, numerical modelling suggests that polar type ice sheets of Laurentide dimensions would wax and wane at Bond cycle periods of about 6-7 ka without external forcing (Ghil 1988, Cutler et al. 1998). However, some of these trigger mechanisms may have been active also during non-glacial times, such as the Holocene. If this is the case, then one should expect a significant glacial event to have occurred both c. 6000 years ago and at the present, since the last ice-age-6ka-cycle occurred about 12,000 years ago (also known as the Younger Dryas event). We know that the expected long-term precession (19 and 23 ka orbital cycles) induced growth of large ice sheets at about 6000 years BP failed to take place. This is explained by the very high contents of CO_2 and CH_4 in the atmosphere that continued to be at high levels, although the solar radiation has decreased at northern latitudes during the entire Holocene (Berger & Loutre 1991). Furthermore, the summer temperature represented by SST data from the fjord region of northern Norway has decreased steadily over the last 6000 years (Birks & Koc 2002), which were quite different from previous cold episodes as inferred from ice-core records (e.g., Ruddiman 2003).

However, significant ice growth did, in fact, occur at around 6000 years BP. Studies of some of the largest of the 3000 small glaciers that occur in Fennoscandia today indicate that the majority of these started to grow shortly after 6000 years ago (e.g., Nesje & Dahl 1993, Dahl & Nesje 1994, Gunnarsdóttir 1996, Nesje et al. 2000a, b, Barnett et al. 2001, Larsen et al. 2003). Most of these glaciers had a maximum extension during the Holocene barely a hundred years ago, but also had significant variations in the intervening periods. The ice-age 6ka-climatic-cycle that we have discussed may therefore include non-glacial intervals like the Holocene, although the amplitude of the variations is obviously much smaller during such non-glacial times.

Some of the most important triggering mechanisms for the discussed climatic cycles may be the same both prior to and during the Holocene. The precession-induced cycles will co-vary approximately with every third 6-ka-cycle and may therefore strengthen these events during glacial times. Some of the solar activity 1-2 ka quasi-cycles will probably also co-vary with the 6-ka-cycles and thus affect these to a certain extent.

It is beyond the scope of this paper to discuss the effect of any of the internal forcing factors in detail. However, the many possible mechanisms involved may function as a reminder of the complexity of natural climatic changes, not to mention the increased complexity if anthropogenic climatic changes are also added on top of the natural signal (see for example, IPCC 2001).

Conclusions

Previously, we have shown that between 11 and 45 (^{14}C) ka BP semi-cycles of glacial fluctuations comparable to the Bond cycle bundles of DO cycles are recorded from both marine and terrestrial data from Norway, hosting the western part of the Fennoscandian ice sheet (Olsen 1997, Olsen et al. 2001a, b, c, 2002).

We have here presented and discussed further the cyclical nature of these fluctuations, as represented by the distribution of 264 dates from ice-free periods separated by glacial advances during the age interval 12-50 ka BP from this area. From spectral analysis and autocorrelation we conclude that these fluctuations follow a cyclic pattern of 6 ka length. The resulting autocorrelation peak is statistically significant at $p<0.05$, referring to a 95% confidence interval. The fluctuations describe a more semi-cyclic pattern at higher significance levels, and this is what should be expected from the variety of materials and dates, and the proportion (1/3) of samples with low organic carbon content that are included. The possible narrow spike character of the climatic variations that we have recorded is difficult to test statistically, and even using autocorrelation, which may be the best available method to test such variations, the cyclical nature of the data may be better than we have found.

Comparison between our results and other proxy climatic records of cyclical nature from different parts of the world (from ice cores, marine sediments, speleothems, loess, sea-level data, etc.) suggests a global link between these data. We conclude that during the glacial periods, ice sheets were clearly involved as the most likely causes of such cyclic changes. Sea-level rise is probably the most important synchronizing factor for the timing of the retreat of marine-based ice sheets. During the Holocene a 6 ka-cycle is possibly still present, but less distinct and resulting from other mechanisms, possibly including external factors.

Acknowledgements

The main basis for this paper is several years of regional Quaternary geological mapping and stratigraphical fieldwork funded by the Geological Survey of Norway (NGU). Jan Mangerud, Atle Nesje and Tom Segalstad have reviewed the manuscript, and David Roberts has corrected the English text. We are grateful to all these persons who have contributed with critical comments which have improved the final version.

References

Altabet, M.A., Higginson, M.J., & Murray, D.W. 2002: The effect of millennialscale changes in Arabian Sea denitrification on atmospheric CO_2. *Nature 415,* 159–162.

Barber, D.C., Dyke, A., Hillaire-Marcel, C.; Jennings, A.E., Andrews, J.T., Kerwin, M.W., Bilodeau, G., McNeely, R., Southon, J., Morehead, M.D. & Gagnon, J.-M. 1999: Forcing of the cold event of 8,200 years ago by catastrophic drainage of Laurentide lakes. *Nature 400*, 344–348.

Barnett, C., Dumayne-Peaty, L. & Matthews, J.A. 2001: Holocene climatic change and tree-line response in Leirdalen, central Jotunheimen, south central Norway. *Review of Palaeobotany and Palynology 117*, 119–137.

Beer, J., Mende, W. & Stellmacher, R. 2000: The role of the sun in climate forcing. *Quaternary Science Reviews 19*, 403–415.

Beer, J., Muscheler, R., Wagner, G., Laj, C., Kissel, C., Kubik, P.W. & Synal, H-A. 2002: Cosmogenic nuclides during isotope stages 2 and 3. *Quaternary Science Reviews 21*, 1129–1139.

Benson, L., Lund, S., Negrini, R., Linsley, B. & Zic, M. 2003: Response of North American Great Basin Lakes to Dansgaard-Oeschger oscillations. *Quaternary Science Reviews 22*, 2239–2251.

Berger; A. & Loutre, M.F. 1991: Insolation values for the climate of the last 10 million years. *Quaternary Science Reviews 10*, 297–317.

Birks, J. & Koc, N. 2002: A high-resolution diatom record of late Quaternary sea-surface temperatures and oceanographic conditions from the eastern Norwegian Sea. *Boreas 31*, 323–344.

Bjune, A., Nesje, A., Birks, J., Andersson Dahl, A., Seppä, H. & Jansen, E. 2003: Mer pålitelige rekonstruksjoner av fortidens klima: bedre forståelse av naturlige klimaendringer i fortiden vil gi bedre modeller for framtidens klima. *Cicerone 4,* 2003, 27–28.

Bond, G., Broecker, W.S., Johnsen, S., McManus, J., Labeyrie, L., Jouzel, J. & Bonani, G. 1993: Correlations between climate records from the North Atlantic sediments and Greenland ice. *Nature 365*, 143–147.

Bond, G., Kromer, B., Beer, J., Muscheler, R., Evans, M.N., Showers, W., Hoffmann, S., Lotti-Bond, R., Hajdas, I. A. & Bonani, G. 2001: Persistent Solar Influence on North Atlantic Climate During the Holocene. *Science 294*, 2130–2136.

Boulton, G.S. 1993: Two cores are better than one. *Nature 366*, 507–508.

Broecker, W.S. 1998: Paleocean circulation during the last deglaciation: A bipolar seesaw? *Paleoceanography 13*, 119–121.

Broecker, W.S. 2000: Abrupt climate change: causal constraints provided by the paleoclimate record. *Earth-Science Reviews 51*, 137–154.

Broecker, W.S., Bond, G., Klas, M., Clark, E. & McManus, J. 1992: Origin of the northern Atlantic's Heinrich events. *Climate Dynamics 1992*, 265–273.

Cacho, I., Grimalt, J.O., Pelejero, C., Canals, M., Sierro, F., Flores, J.A. & Shackleton. N.J. 1999: Dansgaard-Oeschger and Heinrich event imprints in Alboran Sea paleotemperatures. *Paleoceanography 14*, 698–705.

Chappell, J. 2002: Sea level changes forced ice breakouts in the Last Glacial cycle: new results from coral terraces. *Quaternary Science Reviews 21*, 1229–1240.

Cutler, P.M., MacAyeal, D.R., Colgan, P.M. & Mickelson, D.M. 1998: A numerical investigation of factors influencing the occurrence of millennial scale oscillations of the southern Laurentide Ice Sheet. *Geological Society of America, Abstracts with Programs, v. 30*, 112.

Dahl-Jensen, D., Morgan, V.I. & Elcheikh, A. 2000: Monte Carlo inverse modelling of the law dome (Antarctica) temperature profile. *Annals of Glaciology 29*, 145–150.

Dahl, S.O. & Nesje, A. 1994: Holocene glacier fluctuations at Hardangerjøkulen, central-southern Norway: a high-resolution composite chronology from lacustrine and terrestrial deposits. *The Holocene 4*, 269–277.

Dansgaard, W., Johnsen, S.J., Clausen, H.B., Dahl-Jensen, D., Gundestrup, N.S., Hammer, C.U., Hvidberg, C.S., Steffensen, J.P., Sveinbjörnsdottir, A.E., Jouzel, J. & Bond, G. 1993: Evidence for general instability of past climate from a 250-kyr ice-core record. *Nature 364*, 218–220.

Davis, J.C. 1986: Statistics and Data Analysis in Geology, 2nd Edition. John Wiley & Sons, New York. 646 pp.

Gentry, D., Blamart, D., Ouahdi, R., Gilmour, M., Baker, A., Jouzel, J. & Van-Exter, S. 2003: Precise dating of Dansgaard-Oeschger climate oscillations in western Europe from stalagmite data. *Nature 421*, 833–837.

Ghil, M. 1988: Deceptively simple models of climate change. In Berger, A., Schneider, S., Duplessy, J.-Cl. (Eds.): *Climate and Geosciences.* Kluwer Academic, Dordrecht, 211–240.

Grootes, P.M., Stuiver, M., Saling, T.L., Mayewski, P.A., Spencer, M.J., Alley, R.B. & Jenssen, D. 1990: A 1400-year oxygen isotope history from the Ross Sea Area, Antarctica. *Annals of Glaciology 14*, 94–98.

Grootes, P.M., Stuiver, M., White, J.W.C., Johnsen, S. & Jouzel, J. 1993: Comparison of oxygen isotope records from the GISP2 and GRIP Greenland ice cores. *Nature 366*, 552–554.

Grootes, P.M. & Stuiver, M. 1997: Oxygen 18/16 variability in Greenland snow and ice with 10^{-3} –to 10^5 –year time resolution. *Journal of Geophysical Research 102*, 26455–26470.

Grønås, S. 2003: Tidligere klimaendringer skyldes sola: på den nordlige halvkule finner man spor av åtte kalde perioder etter siste istid… *Cicerone 4*, 2003, 29–31.

Gunnarsdóttir, H. 1996: Holocene vegetation history in the northern parts of the Gudbrandsdalen valley, south central Norway. Unpubl. Dr. Scient. Thesis No. 8, University of Oslo.

Heinrich, H. 1988: Origin and consequences of cyclic ice rafting in the Northeast Atlantic Ocean during the past 130,000 years. *Quaternary Research 29*, 142–152.

Hendy, I.L., Kennett, J.P., Roark, E.B. & Ingram, B.L. 2002: Apparent synchroneity of submillennial scale climate events beteen Greenland and Santa Barbara Basin, California from 30-10 ka. *Quaternary Science Reviews 21*, 1167–1184.

Hinnov, L.A., Schulz, M & Yiou, P. 2002: Interhemispheric space-time attributes of the Dansgaard-Oeschger oscillations between 100 and 0 ka. *Quaternary Science Reviews 21*, 1213–1228.

Hughen, K.A., Overpeck, J.T., Peterson, L.C. & Trumbore, S. 1996: Rapid climate changes in the tropical Atlantic region during the last deglaciation. *Nature 380*, 51–54.

IPCC (Intergovernmental Panel on Climate Change) 2001: 'Climate Change 2001: The Scientific Basis'. Edited by Houghton, T., et al., Cambridge University Press. 881 pp.

Imbrie, J., Hays, J.D., Martinson, D.G., et al., 1984: The orbital theory of Pleistocene climate: support from a revised chronology of the marine $\delta^{18}O$ record. *In* Berger, A., et al. (Eds.): *Milankovitch and Climate: Understanding the Response to Orbital Forcing*. Reidel, Dordrecht, 269–305.

Jaworowski, Z., Segalstad, T.V. & Ono, N. 1992: Do glaciers tell a true atmospheric CO_2 story? *The Science of the Total Environment 114*, 227–284.

Johnsen, S.J., Clausen, H.B., Dansgaard, W., Fuhrer, K., Gundestrup, N., Hammer, C.U., Iversen, P., Jouzel, J., Stauffer, B. & Steffensen, J.P. 1992: Irregular glacial interstadials recorded in a new Greenland ice core. *Nature 359*, 311–313.

Johnsen, S.J., Dahl-Jensen, D., Gundestrup, N., Steffensen, J.P., Clausen, H.B., Miller, H., Masson-Delmotte, V., Sveinbjörnsdottir, A.E. & White, J. 2001: Oxygen isotope and palaeotemperature records from six Greenland ice-core stations: Camp Century, Dye-3, GRIP, GISP2, Renland and NorthGRIP. *Journal of Quaternary Science 16*, 299–307.

Kennett, J.P., Cannariato, K.G., Hendy, I.L. & Behl, R.J. 2000: Carbon isotopic evidence for methane hydrate instability during Quaternary interstadials. *Geology 27*, 291–294.

Kitagawa, H. & van der Plicht, J. 1998: A 40,000-year varve chronology from Lake Suigetsu, Japan: extension of the ^{14}C calibration curve. *Radiocarbon 40*, 505–515.

Larsen, E., Hald, M. & Birks, J. 2003: Tar temperaturen på fortiden: ved å granske fossiler, isbreer, dryppsteiner og gamle gårdsdagbøker har forskere i prosjektet NORPAST kartlagt fortidens klima i Norge … *Cicerone 4*, 2003, 18–23.

Marchitto, T.M., Curry, W.B. & Oppo, D.W. 1998: Millennial-scale changes in North Atlantic circulation since the last glaciation. *Nature 393*, 557–561.

Nesje, A. & Dahl, S.O. 1993: Lateglacial and Holocene glacier fluctuations and climate variations in western Norway: a review. *Quaternary Science Reviews 12*, 255–261.

Nesje, A., et al. 2000a: Is the North Atlantic Oscillation reflected in Scandinavian glacier mass balance records? *Journal of Quaternary Science 15*, 587–601.

Nesje, A., Dahl, S.O., Andersson, C. & Matthews, J.A. 2000b: The lacustrine sedimentary sequence in Sygneskardvatnet, western Norway: a continuous, high-resolution record of the Jostedalsbreen ice cap during the Holocene. *Quaternary Science Reviews 19*, 1047–1065.

Nesje, A., Matthews, J.A., Dahl, S.O., Berrisford, M.S. & Andersson, C. 2001: Holocene glacier fluctuation of Flatebreen and winter-precipitation changes in the Jostedalsbreen region, western Norway, based on glaciolacustrine sediment records. *The Holocene 11*, 267–280.

Olsen, L. 1997: Rapid shifts in glacial extension characterise a new conceptual model for glacial variations during the Mid and Late Weichselian in Norway. *Norges geologiske undersøkelse Bulletin 433*, 54–55.

Olsen, L., van der Borg, K., Bergstrøm, B., Sveian, H., Lauritzen, S.-E. & Hansen, G. 2001a: AMS radiocarbon dating of glacigenic sediments with low organic content – an important tool for reconstructing the history of glacial variations in Norway. *Norsk Geologisk Tidsskrift 81*, 59–92.

Olsen, L., Sveian, H. & Bergstrøm, B. 2001b: Rapid adjustments of the western part of the Scandinavian ice sheet during the Mid- and Late Weichselian – a new model. *Norsk Geologisk Tidsskrift 81*, 93–118.

Olsen, L., Sveian, H., Bergstrøm, B., Selvik, S.F., Lauritzen, S.-E., Stokland, Ø. & Grøsfjeld, K. 2001c: Methods and stratigraphies used to reconstruct Mid- and Late Weichselian palaeoenvironmental and palaeoclimatic changes in Norway. *Norges geologiske undersøkelse Bulletin 438*, 21–46.

Olsen, L., Sveian, H., van der Borg, K. 2002: Rapid and rhythmic ice sheet fluctuations in western Scandinavia 15-40 Kya – a review. *Polar Research 21*, 235–242.

Olsen, L. & Hammer, Ø. 2004: A 6 ka climatic cycle during the last 50,000 years. *Poster and abstract, Nordic Geological Winter meeting, Uppsala, 2004.*

Percival, D.B. & Walden, A.T. 2000: *Wavelet Methods for Time Series Analysis.* Cambridge University Press, Cambridge.

Peterson, L.C., Haug, G.H., Hughen, K.A. & Röhl, U. 2000: Rapid changes in the hydrologic cycle of the Tropical Atlantic during the last glacial. *Science 290*, 1947–1951.

Porter, S.C. & An, Z. 1995: Correlation between climate events in the north Atlantic and China during the last glaciation. *Nature 375*, 305–308.

Press, W.H., Teukolsky, S.A., Vetterling, W.T. & Flannery, B.P. 1992: *Numerical Recipes in C*. Cambridge University Press, Cambridge. 1020 pp.

Rahmstorf, S. 1994: Rapid climate transitions in a coupled ocean-atmosphere model. *Nature 372*, 82–85.

Rasmussen, T.L., Thomsen, E., van Weering, T.C.E. & Labeyrie, L. 1996: Rapid changes in surface and deep water conditions at the Faeroe Margin during the last 58,000 years. *Paleoceanography 11*, 757–771.

Raunholm, S., Sejrup, H. P. & Larsen, E. 2002: Weichselian sediments at Foss-Eikeland, Jæren (southwest Norway): Sea-level changes and glaciation history. *Journal of Quaternary Science 17*, 241–260.

Ruddiman, W.F. 2003: Orbital insolation, ice volume, and greenhouse gases. *Quaternary Science Reviews 22*, 1597–1629.

Sachs, J.P. & Lehman, S.J. 1999: Covariation of subtropical and Greenland temperatures 60,000 to 30,000 years ago. *Science 286*, 756–759.

Schulz, M., Berger, W.H., Sarnthein, M. & Grootes, P.M. 1999: Amplitude variations of 1470-year climate oscillations during the last 100,000 years linked to fluctuations of continental ice mass. *Geophysical Research Letters 26*, 3385–3388,

Stuiver, M., Grootes, P.M. & Braziunas, T.F. 1995: The GISP2 ^{18}O climate record of the past 16,500 years and the role of the sun, ocean and volcanoes. *Quaternary Research 44*, 341–354.

Stuiver, M., Reimer, P.J., Bard, E., Beck, J.W., Burr, G.S., Hughen, K.A., Kromer, B., McGormac, G., van der Plicht, J. & Spurk, M. 1998: INTCAL98 Radiocarbon age calibration 24,000-0 cal. BP. *Radiocarbon 40*, 1041–1083.

Stuiver, M. & Grootes, P.M. 2000: GISP2 oxygen isotope ratios. *Quaternary Research 53*, 277–284.

Stuiver, M. & Quay, P.D. 1980: Changes in atmospheric carbon-14 attributed to a variable sun. *Science 207*, 11–19.

Swan, A.R.H. & Sandilands, M. 1995: Introduction to Geological Data Analysis. Blackwell Science. 446 pp.

Tada, R. & Irino, T. 1999: Land-ocean linkages over orbital and millennial time scales recorded in Late Quaternary sediments of the Japan Sea. *Paleoceanography 14*, 236–247.

van Kreveld, S., Sarnthein, M., Erlenkeuser, H., Grootes, P. Jung, S., Nadeau, M.J., Pflaumann, U. & Voelker, A. 2000: Potential links between surging ice sheets, circulation changes, and the Dansgaard-Oeschger cycles in the Iminger Sea, 60-18 kyr. *Paleoceanography 15*, 425–444.

Wagner, G., Beer, J., Laj, C., Kissel, C., Masarik, J., Muscheler, R. & Synal, H.-A. 2000: Chlorine-36 evidence for the Mono Lake event in the Summit GRIP ice core. *Earth and Planetary Science Letters 181*, 1–6.

Wang, Y.J., Cheng, H., Edwards, R.L., An, Z.S., Wu, J.Y., Shen, C.-C. & Dorale, J.A. 2001: A high-resolution absolute-dated late Pleistocene monsoon record from Hulu Cave, China. *Science 294*, 2345–2348.